Stabilizing Mixed Traffic with Minimal AV Control

Niclas Scheuer
nscheuer@ethz.ch

***Abstract*—The stability and control of traffic flow in a ring road system comprising identical human driven vehicles (HDVs) is studied. We adopt a modified predecessor following (PF) Helly's model and express the system in terms of headway deviations. The stability of the interconnection is evaluated as a function of vehicle gains and fleet size. Specifically, we show that that strong-frequency domain ring stability (SFSS) using the small-gain theorem is stricter than interconnection stability conditions. We demonstrate that the system is stabilizable by introducing one autonomous vehicle (AV) and implement a Linear Quadratic Regulator (LQR) controller in simulation.**

***Index Terms*—traffic dynamics, autonomous vehicle, Helly's model, ring stability**

I. Introduction

Stop-and-go traffic is a common inefficiency when considering traffic systems. It may arise due to bottlenecks on the road or in the absence of any bottlenecks. Sugiyama et al. famously demonstrate the creation and propagation of traffic waves in an experimental, bottleneck-free setting involving 22 human drivers on a ring road [1]. Such self-induced congestion highlights the limitations of human driving behavior in maintaining stable traffic flow. The growing integration of autonomous vehicles (AVs) into a mixed traffic flow with human drivers therefore offers new opportunities for reducing traffic congestion and fuel consumption.

To describe traffic dynamics, various car-following models have been developed and are well-represented in the literature. Specifically, microscopic traffic models deal with individual car dynamics. In this field, Pipes' model (1953) first introduced a traffic scheme in which drivers maintain a safe distance proportional to their speed [2]. Helly's model (1959) built on this by introducing relative velocity as a factor [3]. These efforts culminated in the Gazis-Herman-Rothery (GHR) model (1961), which included a headway-dependent sensitivity and appropriate reaction time delays [4]. Nonlinear models such as the Optimal Velocity (OV) model (1995) introduced the notion of prescribing an equilibrium speed as a function of headway [5]. Many more traffic flow models can be found in the model tree created by van Wageningen-Kessels et al. [6]. Among these, Helly's model remains a key linear approximation of OV-type models, as derived in [7], proving particularly practical for stability analyses via Lyapunov's indirect method. In this paper, we adopt a modified Helly's model that enforces a desired headway and a prescribed speed limit.

For a long time, it was believed that significant improvements in traffic flow would require a high penetration of connected or autonomous vehicles [8] [9]. However, advances in traffic flow theory and autonomous vehicle control have revealed that even a small number of AVs can improve stability and efficiency. Stern et al. experimentally demonstrated that controlling a single autonomous vehicle in a mixed-traffic ring road can dissipate stop-and-go waves, demonstrating flow control is possible with as little as 5% AVs in mixed traffic [10]. Building on this, Zheng et al. [11] proved that an N HDV Helly's model is stabilizable with a single AV, and implemented a controller that boasts 6% traffic speed improvement at only 5% penetration rate. Furthermore, Giammarino et al. [7] show, under a similar Helly-type model with typical human-driver gains, approximately 25% AV penetration is required to ensure string stability.

In this paper, we use a modified Helly's model to represent drivers on a ring road, modeling drivers' tendency to maintain a set headway and speed limit. We first derive stability regions for headway and velocity gains based on the notion of strong frequency-domain string stability (SFSS) using the $\mathcal{H}_\infty$-norm and the small-gain theorem, yielding conditions that, while independent of fleet size N, are conservative. Next, we exploit the properties of circulant matrices to characterize interconnection stability of the whole system in terms of model gains and fleet size. We show that the SFSS stability region is completely contained within the interconnection stability region for any fleet size N. We then demonstrate that introducing a single AV renders the system stabilizable, and design a stabilizing LQR controller. Finally, simulation results illustrate the effectiveness of the proposed controller in dissipating stop-and-go waves and improving traffic flow.

The remainder of this paper is organized as follows. Section II introduces the mathematical preliminaries, notation, and key definitions. Section III presents the problem formulation and control objectives. Section IV develops the theoretical analysis, including stability region derivation, stabilizability conditions, and the formulation of the the LQR controller. Section V reports numerical simulations under various vehicle configurations, comparing scenarios with and without control. Finally, Section VI concludes the paper and discusses directions for future work.

II. Mathematical Preliminaries

A continuous-time linear time-invariant (LTI) takes the form:

$$\dot{x}(t) = Ax(t) + Bu(t), \quad x(0) = x_0,$$

where $x(t) \in \mathbb{R}^{n\times 1}$ is the state vector, $u(t) \in \mathbb{R}^{m\times 1}$ is the input vector, $A \in \mathbb{R}^{n\times n}$ is the system matrix, and $B \in \mathbb{R}^{n\times m}$ is the input matrix.

Given matrices $A \in \mathbb{R}^{m\times n}$ and $B \in \mathbb{R}^{p\times q}$, their Kronecker product $A \otimes B \in \mathbb{R}^{mp\times nq}$ is defined as

$$A \otimes B = \begin{bmatrix} a_{11}B & \cdots & a_{1n}B \\ \vdots & \ddots & \vdots \\ a_{m1}B & \cdots & a_{mn}B \end{bmatrix}.$$

Furthermore, we define the following notations:

T^*	The conjugate transpose (Hermitian transpose) of a complex matrix T.
$\mathbb{I}_k$	The $k \times k$ identity matrix.
$\mathbf{1}_k$	The $k \times 1$ vector of ones.
e_k	The kth standard basis vector, i.e., a vector with a 1 in the kth position and zeros elsewhere.

A directed graph (or digraph) is denoted by $\mathcal{G} = (\mathcal{V}, \mathcal{E}, A)$, where:

- $\mathcal{V} = \{1, 2, \ldots, N\}$ is the set of nodes (vehicles),
- $\mathcal{E} \subseteq \mathcal{V} \times \mathcal{V}$ is the set of directed edges,
- $A \in \{0, 1\}^{N\times N}$ is the adjacency matrix, where $[A]_{ij} = 1$ if and only if $(j \to i) \in \mathcal{E}$, and 0 otherwise.

Theorem II.1 (Continuous Time LTI Stability Theorem, [12])**.** *Consider the continuous-time LTI system: $\dot{x} = Ax$*

- *The system is* asymptotically stable *if and only if all eigenvalues λ_i of A have real part $\sigma_i < 0$.*
- *The system is* stable *if some of its eigenvalues λ_k of A have real part $\sigma_k = 0$ but no eigenvalue λ_i has $\sigma_i > 0$.*

Theorem II.2 (Continuous-Time Controllability, [13])**.** *The continuous-time LTI system $\dot{x} = Ax + Bu$, $A \in \mathbb{R}^{n\times n}$, $B \in \mathbb{R}^{n\times m}$ is controllable if and only if:*

$$\textit{rank}[B, AB, A^2B, \ldots, A^{n-1}B] = n$$

Theorem II.3 (Invariance under Linear Transformation, [14])**.** *Let $A \in \mathbb{R}^{n\times n}$, $B \in \mathbb{R}^{n\times m}$, and let $T \in \mathbb{R}^{n\times n}$ be a nonsingular matrix. Then:*

1) *The eigenvalues of A are invariant under similarity transformation, i.e.,*

$$\textit{spec}(A) = \textit{spec}(T^{-1}AT).$$

2) *Controllability is preserved under similarity transformation:*

$$(A, B) \textit{ controllable} \iff (T^{-1}AT, T^{-1}B) \textit{ controllable.}$$

Theorem II.4 (Block-Circulant Diagonalization, [15])**.** *Let $A \in \mathbb{C}^{kn\times kn}$ be block-circulant with blocks of size $k \times k$, $A = \textit{circ}(C_0, C_1, \ldots, C_{n-1})$. Using $j = \sqrt{-1}$, define the unitary discrete Fourier matrix:*

$$(F_n)_{ik} = \frac{1}{\sqrt{n}}\omega_n^{(i-1)(k-1)}, \quad \omega_n = e^{-\frac{2\pi j}{n}}, \quad j, k \in 1, \ldots, n.$$

and set $T = F_n^* \otimes I_k$. Then T is nonsingular and:

$$\tilde{A} = T^{-1}AT = \textit{diag}(D_0, D_1, \ldots, D_{n-1}).$$

with diagonal blocks:

$$D_l = \sum_{k=0}^{n-1} C_k \omega_n^{lk} \quad l = 0, \ldots, n-1.$$

Theorem II.5 ($\mathcal{H}_\infty$-norm of Multi-Input Multi-Output (MIMO) system, [14], (3.34), (9.42))**.** *For a MIMO system with transfer function $G(s) = C(s\mathbb{I} - A)^{-1}B + D \in \mathbb{R}^{n\times m}$, the $\mathcal{H}_\infty$-norm is given by:*

$$||G||_{\mathcal{H}_\infty} = \sup_{\omega>0} \sqrt{|\lambda_{max}(G^*(j\omega)G(j\omega))|}$$

Theorem II.6 (Strong-Frequency Domain String Stability, [16])**.** *A linear platoon system is considered strong-frequency domain string stable (SFSS) if the transfer function between vehicle i and its predecessor $i-1$ satisfies:*

$$||G_{i-1,i}||_{\mathcal{H}_\infty} \leq 1, \quad \forall i.$$

III. Problem Formulation

In this section, we formulate the traffic dynamics problem first for a single vehicle. We begin by describing the behaviour of a single vehicle and expand the analysis to N vehicles in a ring network. Building on this, we construct stacked systems in terms of the absolute vehicle states (position, velocity) and relative vehicle states (distance, velocity difference) to analyze the stability of the system. Finally, we introduce a single input to simulate the control law of an AV.

A. Individual Dynamics

Consider the description of a vehicle as a second-order integrator system.

$$\begin{bmatrix} x_i \\ \dot{x}_i \end{bmatrix}' = \begin{bmatrix} 0 & 1 \\ 0 & 0 \end{bmatrix} \begin{bmatrix} x_i \\ \dot{x}_i \end{bmatrix} + \begin{bmatrix} 0 \\ u_i(t) \end{bmatrix} \tag{1}$$

The intention of the driver is to respond to stimulus from other vehicles and the road via the acceleration of their own vehicle $u_i(t)$. We model the driver as tracking a fixed velocity v_{ref}, which may be a speed limit or desired cruising speed, and maintaining a fixed distance to the car ahead. This leads to the driver control law:

$$u_i(t) = \alpha(v_{ref} - \dot{x}_i(t)) + \beta(x_{i-1}(t) - d - x_i), \quad \alpha, \beta > 0 \tag{2}$$

Combinining equations (1) and (2) yields a modified version of Helly's model:

$$\begin{bmatrix} x_i \\ \dot{x}_i \end{bmatrix}' = \begin{bmatrix} 0 & 1 \\ -\beta & -\alpha \end{bmatrix} \begin{bmatrix} x_i \\ \dot{x}_i \end{bmatrix} + \begin{bmatrix} 0 & 0 \\ \beta & 0 \end{bmatrix} \begin{bmatrix} x_{i-1} \\ \dot{x}_{i-1} \end{bmatrix} + \begin{bmatrix} 0 \\ \alpha v_{ref} - \beta d \end{bmatrix} \tag{3}$$

B. Stacked Dynamics

Consider now a group of N vehicles using dynamics (3) on a one-lane ring road of circumference $L = Nd$. To capture the information flow topology [16], we introduce the directed graph $\mathcal{G} = (\mathcal{V}, \mathcal{E}, \mathcal{A})$, where

- $\mathcal{V} = \{1, 2, \ldots, N\}$ is the set of vertices, each corresponding to one vehicle,
- $\mathcal{E} = (i - 1 \to i)_{i=1}^{N}$ with indices modulo N since each driver i receives information only from the driver $i - 1$ ahead.
- $\mathcal{A}_{ij} = \begin{cases} 1, & \text{if } j = i - 1 \mod(N) \\ 0, & \text{otherwise} \end{cases}$

By definition of $\mathcal{A}$, each node i has a directed edge from $i-1$, with indices taken modulo N. As a result, starting from any node i, one can reach any other node j by traversing the directed ring in at most $N-1$ steps. Therefore, the graph is strongly connected.

Since the graph $\mathcal{G}$ is a strongly connected, circulant digraph, any perturbation from one vehicle will eventually influence any other vehicle.

Using the adjacency matrix $\mathcal{A}$, we are able to stack the dynamics of all N vehicles into the following LTI system with a constant disturbance term:

$$\dot{X} = AX + (\alpha v_{ref} - \beta d)\mathbf{e} \tag{4}$$

where:

- $X = \begin{bmatrix} x_1 & \dot{x}_1 & x_2 & \dot{x}_2 & \cdots & x_N & \dot{x}_N \end{bmatrix}^\intercal$
- $A = \mathbb{I}_N \otimes \begin{bmatrix} 0 & 1 \\ -\beta & -\alpha \end{bmatrix} + \mathcal{A} \otimes \begin{bmatrix} 0 & 0 \\ \beta & 0 \end{bmatrix}$
- $\mathbf{e} = \mathbf{1}_N \otimes \begin{bmatrix} 0 & 1 \end{bmatrix}^\intercal$

For ease of notation, we define henceforth:

$$A_0 = \begin{bmatrix} 0 & 1 \\ -\beta & -\alpha \end{bmatrix} \quad B_0 = \begin{bmatrix} 0 & 0 \\ \beta & 0 \end{bmatrix}$$

C. Stacked Headway Dynamics

For stability analysis and later control of the system, we remove the constant forcing term $(\alpha v_{ref} - \beta d)\mathbf{e}$ by rewriting the system in terms of relative vehicle headway $s_i = x_{i-1} - x_i$, $\dot{s}_i = \dot{x}_{i-1} - \dot{x}_i$. Using the stacked headway state vector $S = \begin{bmatrix} s_1 & \dot{s}_1 & s_2 & \dot{s}_2 & \cdots & s_N & \dot{s}_N \end{bmatrix}^\intercal$, we can express the system as:

$$\dot{S} = AS \tag{5}$$

where A is identical to the one used in equation (4).

D. Control Input and Objective

The goal is to analyse the stability properties of the ring road dynamics and design a control strategy for a minimal number of AVs to stabilize the system. Specifically, we aim to:

1) Characterize the stability of the system as a function of the parameters α, β, and N.
2) Determine conditions under which the system is stabilizable.
3) Synthesize a controller to stabilize the interconnection.

IV. Results

A. Strong Frequency Domain String Stability (SFSS)

Strong Frequency Domain String Stability (SFSS) is the notion that perturbations are not amplified between consecutive vehicles.

Theorem IV.1 (SFSS Stability of the Ring Model)**.** *Consider the traffic model on a ring road given by* (4)*. The system is strong frequency domain stable if:*

$$\beta \leq -1 + \sqrt{\alpha^2 + 1} \tag{6}$$

Proof. By using notation $X_i = \begin{bmatrix} x_i & \dot{x}_i \end{bmatrix}$, we are able to perform a Laplace transform on the system (3) to find the transfer function along the edge of the graph $\mathcal{G}$ to be:

$$G_{i-1,i}(s) = \frac{X_i(s)}{X_{i-1}(s)} = \frac{\beta}{s^2 + \alpha s + \beta} \begin{bmatrix} 1 & 0 \\ s & 0 \end{bmatrix} \tag{7}$$

Using the definition of the $\mathcal{H}_\infty$-norm for MIMO systems from Theorem II.5:

$$||G_{i-1,i}(s)||_{\mathcal{H}_\infty} = \sup_{\omega > 0} \frac{\beta\sqrt{1+\omega^2}}{\sqrt{\left(\beta - \omega^2\right)^2 + \alpha^2\omega^2}} \tag{8}$$

Applying the condition for SFSS stability from Theorem II.6 and solving yields the aforementioned condition. □

Lemma IV.2 (Stability of the Ring Model via Small Gain)**.** *If appropriate gains (α, β) are chosen such that Theorem IV.1 holds, then each edge between vehicles on the graph has an $\mathcal{H}_\infty$-gain ≤ 1. The ring road can be represented as a unity-feedback interconnection of these blocks in series. By the Small Gain Theorem, the loop gain satisfies $\gamma = \prod_{i=1}^{N} ||G_{i-1,i}||_{\mathcal{H}_\infty} \leq 1$, which guarantees that the closed-loop system is stable.*

B. Eigenvalue Stability

While SFSS ensures that local interactions do not amplify disturbances, reliance of the Small Gain Theorem renders it a conservative condition. To obtain global stability, we investigate the eigenvalue stability of the stacked system (4).

Theorem IV.3 (Eigenvalue Stability of the Ring Model)**.** *Consider the traffic model on a ring road given by* (4)*. The system is stable if:*

$$\beta \leq \frac{\alpha^2}{2\cos^2\left(\frac{\pi}{N}\right)} \tag{9}$$

Proof. First, we exploit the fact that matrix A in (4) is a circulant Block-Toeplitz matrix, namely $A = \text{circ}(A_0, 0, \ldots, 0, B_0)$. Performing a Fourier Diagonalization (Theorem II.4):

$$\tilde{A} = T^{-1}AT = \text{diag}(\tilde{D}_0, \tilde{D}_1, ..., \tilde{D}_{N-1}) \tag{10}$$

$$\tilde{D}_l = A_0 + \omega_N^{l(N-1)} B_0 = A_0 + e^{\frac{2\pi jl}{N}} B_0 \tag{11}$$

Since the eigenvalues of A are equivalent to those of $\tilde{A}$ (Theorem II.3), we may now use the resultant block-diagonal form of $\tilde{A}$ to find the eigenvalues:

$$\lambda(A) = \bigcup_{l=0}^{N-1} \left\{ -\frac{\alpha}{2} \pm \frac{1}{2}\sqrt{\alpha^2 - 4\beta\left(1 - e^{\frac{2\pi jl}{N}}\right)} \right\} \tag{12}$$

By inspection, $l = 0$ always yields eigenvalues $\lambda_\pm(D_0) = \{-\alpha, 0\}$. Among $l \neq 0$, $l = 1$ yields the eigenvalues with the largest real part, and thus determines the stability condition (Theorem II.1):

$$\text{Re}[\lambda_+(\tilde{D}_1)] \leq 0; \tag{13}$$

Applying the identity $\mathrm{Re}[\sqrt{X+jY}] = \mathrm{Re}[\sqrt{\frac{\sqrt{X^2+Y^2}+X}{2}}]$:

$$\beta \sin^2\left(\frac{2\pi}{N}\right) \leq \alpha^2\left(1-\cos\left(\frac{2\pi}{N}\right)\right) \tag{14}$$

Finally, using the trigonometric identities $1-\cos(2\theta) = 2\sin^2(\theta)$ and $\sin(2\theta) = 2\sin(\theta)\cos(\theta)$ yields the intended inequality. □

Lemma IV.4 (SFSS Region ⊂ Eigenvalue Stable Region)**.** *Consider the traffic model on a ring road given by* (4)*. Let*

$$\mathcal{R}_{SFSS} = \left\{(\alpha,\beta) | \beta \leq -1+\sqrt{\alpha^2+1}\right\} \tag{15}$$

denote the stability region from Theorem IV.1, and

$$\mathcal{R}_{eig} = \left\{(\alpha,\beta) | \beta \leq \frac{\alpha^2}{2\cos^2\left(\frac{\pi}{N}\right)}\right\} \tag{16}$$

denote the stability region from Theorem IV.3. Then:

$$\mathcal{R}_{SFSS} \subset \mathcal{R}_{eig} \quad \forall N \geq 3 \tag{17}$$

Proof. Since $\cos\left(\frac{\pi}{N}\right) \leq 1$ for all $N \geq 3$, we have:

$$-1+\sqrt{\alpha^2+1} \leq \frac{\alpha^2}{2} \leq \frac{\alpha^2}{2\cos^2\left(\frac{\pi}{N}\right)} \tag{18}$$

□

C. Controllability Analysis

The previous sections have shown that not all choices of gains (α,β) under dynamics (4) yield a stable ring-road system. Additionally, even when the system is stable, complex eigenvalues in A can lead to oscillatory traffic waves. To mitigate these effects, we explore whether a single controlled AV can improve overall system behavior.

To achieve this, we augment the system (4) with one input:

$$\dot{X} = AX + (\alpha v_{ref} - \beta d)\mathbf{e} + B_x v \tag{19}$$

where $B_x = \begin{bmatrix}\mathbf{0}_{2\times 1} & \cdots & \mathbf{0}_{2\times 1} & \begin{bmatrix}0 & 1\end{bmatrix}^\intercal\end{bmatrix}^\intercal$

Applying this same input to the system in headway form (5), yields:

$$\dot{S} = AS + B_s v \tag{20}$$

where $B_s = \begin{bmatrix}\begin{bmatrix}0 & 1\end{bmatrix}^\intercal & \mathbf{0}_{2\times 1} & \cdots & \mathbf{0}_{2\times 1} & \begin{bmatrix}0 & -1\end{bmatrix}^\intercal\end{bmatrix}^\intercal$

Theorem IV.5 (Controllability with one AV)**.** *The mixed traffic system* (19) *is controllable for all values of* (α,β)*.*

Proof. We first perform the Fourier diagonalization on the system (19). This yields the same $\tilde{A} = T^{-1}AT$ as in Theorem IV.3, but with the input matrix:

$$\tilde{B}_x = T^{-1}B_x = (F_N^* \otimes \mathbb{I}_2)(e_n \otimes e_2) \tag{21}$$
$$= (F_N^* e_N) \otimes e_2 \tag{22}$$
$$= \frac{1}{\sqrt{N}}\begin{bmatrix}1 & \omega_N^{N-1} & \omega_N^{2(N-1)} & \cdots & \omega_N^{(N-1)(N-1)}\end{bmatrix}^\intercal \otimes e_2 \tag{23}$$
$$= \frac{1}{\sqrt{N}}\begin{bmatrix}1 & \omega_N^{-1} & \omega_N^{-2} & \cdots & \omega_N^{-(N-1)}\end{bmatrix}^\intercal \otimes e_2 \tag{24}$$
$$= \frac{1}{\sqrt{N}}\begin{bmatrix}0 & 1 & 0 & \omega_N^{-1} & \cdots & 0 & \omega_N^{-(N-1)}\end{bmatrix}^\intercal \tag{25}$$
$$= \begin{bmatrix}E_0 & \cdots & E_{N-1}\end{bmatrix}^\intercal \tag{26}$$

The linear transformation T yields N independent 2×2 subsystems:

$$\dot{\tilde{x}}_l = \tilde{D}_l \tilde{x}_l + \tilde{E}_l v, \quad l = 0,\ldots,N-1 \tag{27}$$

$$\tilde{D}_l = \begin{bmatrix}0 & 1\\ -\beta(1-\omega_N^l) & -\alpha\end{bmatrix}, \quad \tilde{E}_l = \frac{\omega_N^{-l}}{\sqrt{N}}\begin{bmatrix}0\\1\end{bmatrix} \tag{28}$$

As it turns out, the controllability matrix of each subsystem is:

$$\mathcal{R} = \frac{\omega_N^{-l}}{\sqrt{N}}\begin{bmatrix}0 & 1\\ 1 & -\alpha\end{bmatrix} \tag{29}$$

and therefore full rank for any (α,β,l). Using Theorem II.3, we conclude that the system (19) is likewise controllable for any (α,β). □

Theorem IV.6 (Controllability of headway dynamics with one AV)**.** *The mixed traffic system in headway form* (20) *is not controllable. However, it is stabilizable for all values of* (α,β)*.*

Proof. As in the proof for Theorem IV.5, we perform the Fourier diagonalization on the system (20). This yields the same $\tilde{A} = T^{-1}AT$ as in Theorem IV.3, but with the input matrix:

$$\tilde{B}_s = T^{-1}B_s = (F_N^* \otimes \mathbb{I}_2)((e_1 - e_N) \otimes e_2) \tag{30}$$
$$= (F_N^*(e_1 - e_N)) \otimes e_2 \tag{31}$$
$$= \frac{1}{\sqrt{N}}\begin{bmatrix}0 & 1-\omega_N^{-1} & 1-\omega_N^{-2} & \cdots & \omega_N^{-(N-1)}\end{bmatrix}^\intercal \otimes e_2 \tag{32}$$
$$= \frac{1}{\sqrt{N}}\begin{bmatrix}0 & 0 & 0 & 1-\omega_N^{-1} & \cdots & 0 & \omega_N^{-(N-1)}\end{bmatrix} \tag{33}$$
$$= \begin{bmatrix}E_0 & \cdots & E_{N-1}\end{bmatrix}^\intercal \tag{34}$$

The linear transformation T similarly yields N independent 2×2 subsystems:

$$\dot{\tilde{x}}_l = \tilde{D}_l \tilde{x}_l + \tilde{E}_l v, \quad l = 0,\ldots,N-1 \tag{35}$$

$$\tilde{D}_l = \begin{bmatrix}0 & 1\\ -\beta(1-\omega_N^l) & -\alpha\end{bmatrix}, \quad \tilde{E}_l = \frac{1-\omega_N^{-l}}{\sqrt{N}}\begin{bmatrix}0\\1\end{bmatrix} \tag{36}$$

By inspection, $l=0$ is the only subsystem that is not controllable. However, from the proof in Theorem IV.3, the associated eigenvalues are always $\lambda_\pm(D_0) = \{-\alpha, 0\}$, which means the system is stabilizable. The remaining $N-1$ subsystems are controllable, and therefore the system (20) is stabilizable for all values of (α,β). □

Remark:
The uncontrollable modes in (20) likely corresponds to the invariance of the total spacing around the ring:

$$\sum_{i=1}^{N} s_i = L \quad \sum_{i=1}^{N} \dot{s}_i = 0 \tag{37}$$

D. LQR Control

Having established the stabilizability of (20), it possible to apply LQR control on a slightly modified formulation. Writing $\delta s_i = s_i - d$ and $\dot{\delta s}_i = \dot{s}_i$, we obtain a regulation problem of form:

$$\delta S = \begin{bmatrix} \delta s_1 & \dot{\delta s}_1 & \delta s_2 & \dot{\delta s}_2 & \cdots & \delta s_N & \dot{\delta s}_N \end{bmatrix}^\intercal \to 0_{2N\times 1}$$

$$\dot{\delta S} = A\delta S + B_s v \tag{38}$$

The matrices A and B_s are unchanged from (20).

V. Numerical Simulation

This section presents numerical simulations to validate the theoretical findings.

For the simulation, we match Sugiyama's [1] setup of $N = 22$ vehicles on a ring road of circumference $L = 230$ m. All vehicles are instructed to travel at $v_{ref} = 8.33$ m/s (30 km/h) and maintain a headway of $d = \frac{L}{N} = 10.45$ m. The system is constrained with a minimum velocity 0 m/s and a maximum velocity 11.11 m/s (40 km/h).

A. Homogeneous System Response

All vehicles but one initially travel at the reference speed v_{ref} and maintain the desired headway d. The system is perturbed by having vehicle 3 travel at 5.33 m/s, instead of 8.33 m/s. This allows us to investigate the system's response for different headway and velocity gains (α, β).

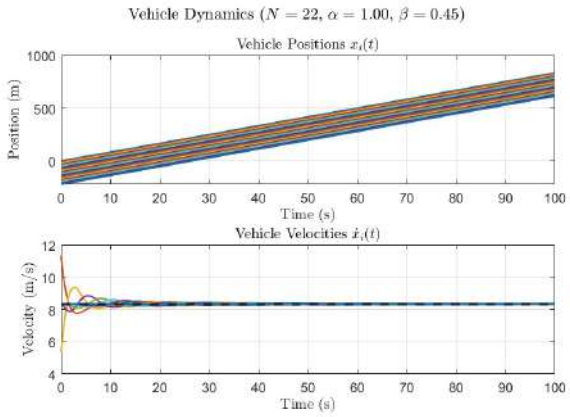

Fig. 1. Example of a stable homogeneous system response with $(\alpha, \beta) = (1.0, 0.45)$. The system returns to the reference speed and headway after a transient period.

Results of a simulation with a pair of stable and unstable gains can be seen in Figures 1 and 2 respectively. In the stable case, the system returns to the reference speed and headway after a transient period. In contrast, the unstable case leads to traffic waves that propagate through the system, mimicking the stop-and-go waves observed in real traffic scenarios. In this unstable regime, the use of a constrained linear system lowers the average vehicle speed across the system.

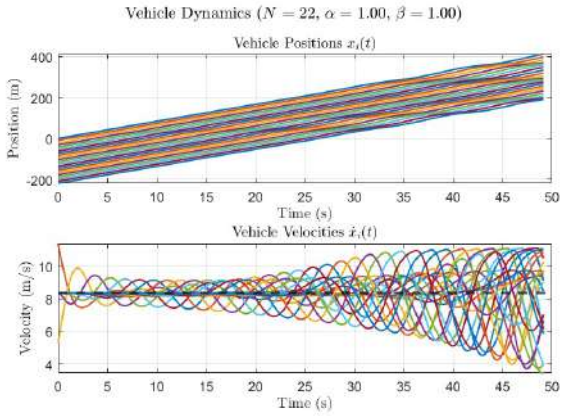

Fig. 2. Example of an unstable homogeneous system response with $(\alpha, \beta) = (1.0, 1.0)$. The initial perturbation leads to traffic waves that propagate through the system.

B. Stability Regions

The SFSS and eigenvalue stability regions were computed manually and compared against the analytical formulas derived in Section IV. The obtained regions are found to be in full agreement with the analytical results and are shown in Figures 3 and 4 respectively. The SFSS region is independent of fleet size N, while the eigenvalue stability region shrinks as N increases, confirming the theoretical predictions.

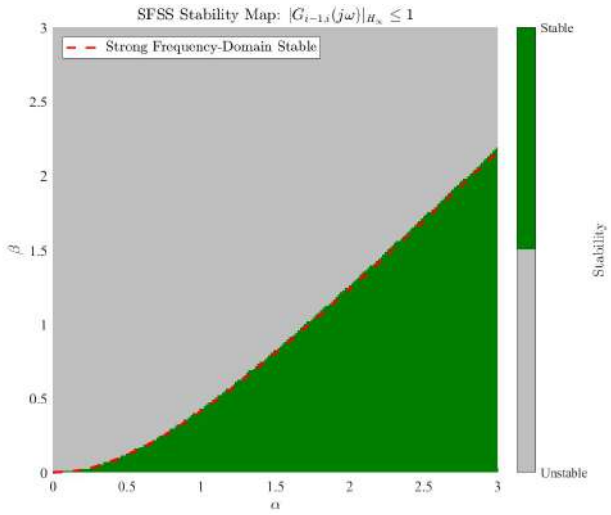

Fig. 3. SFSS stable region on the (α, β)-plane for the homogeneous system. The region is independent of fleet size N. The dashed line corresponds to the boundary derived in Theorem IV.1.

This verifies that for our ring road system, SFSS stability is harder to achieve than eigenvalue stability. Despite using a different model, this aligns with Giammarino et al. [7], who found that string stability demands higher AV gains or penetration than asymptotic stability alone.

C. LQR Control

To demonstrate the effectiveness of stabilizing an unstable ring road system with a single AV, we simulate the system

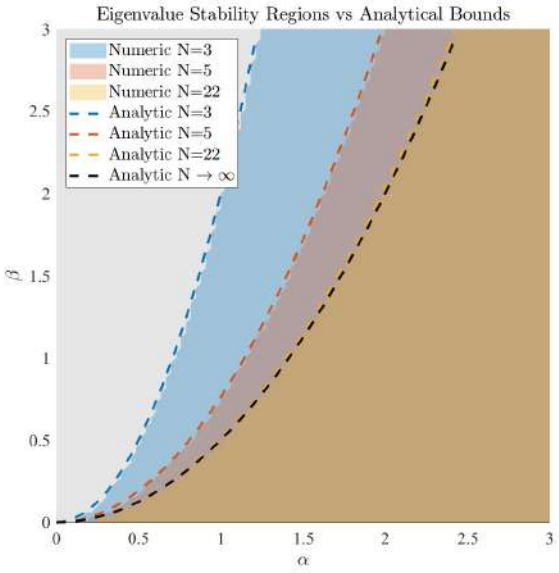

Fig. 4. Eigenvalue stability region on the (α, β)-plane for the homogeneous system. The region shrinks asymptotically with increasing fleet size N. The dashed lines corresponds to the boundary derived in Theorem IV.3.

with the same unstable gains and disturbance as in Figure 2, and the following gains:

$$Q = \mathrm{diag}(1, 1, \ldots, 1) \in \mathbb{R}^{2N \times 2N}, \quad R = 1$$

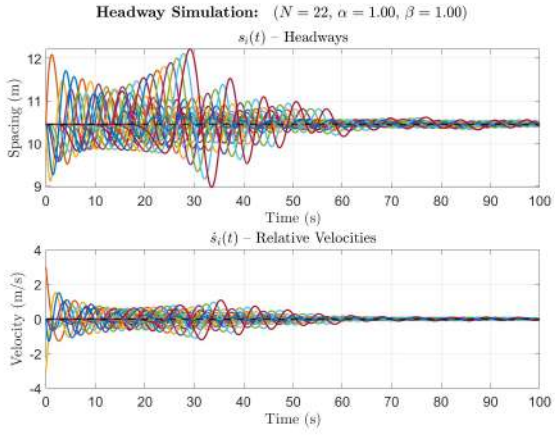

Fig. 5. The LQR controller on one vehicle is able to stabilize the system. The controller is able to dissipate the stop-and-go waves and return all vehicles to the reference speed and headway.

Despite acting on only one vehicle, the LQR controller is able to effectively stabilize an otherwise unstable traffic system. By leveraging feedback from the full state, the controlled AV dissipates stop-and-go waves and restores uniform spacing and velocity across the ring, as shown in Figure 5.

VI. Conclusions

The stability and controllability of a traffic flow system on a ring road was analyzed. Numerical and analytical results show that SFSS is a stricter condition than interconnection stability. Furthermore, it was demonstrated that the system can be regulated using an LQR controller, which was able to stabilize an otherwise unstable system with a single autonomous vehicle (AV). The results suggest that even a small number of AVs can significantly improve traffic flow stability and dissipate stop-and-go waves, highlighting the potential for AVs to enhance traffic efficiency in mixed traffic environments.

The controller proposed has the drawback of requiring full state knowledge. Future work could explore the design of controllers that require only partial state information. Additional research avenues include the use of multiple, collaborating or non-collaborating AVs, and investigating controller robustness against disturbances and noise.

References

[1] Y. Sugiyama *et al.*, "Traffic jams without bottlenecks—experimental evidence for the physical mechanism of the formation of a jam," *New J. Phys.*, vol. 10, p. 033001, Mar. 2008, doi:10.1088/1367-2630/10/3/033001.

[2] L. A. Pipes, "An operational analysis of traffic dynamics," *J. Appl. Phys.*, vol. 24, pp. 274–281, 1953, doi:10.1063/1.1721265.

[3] W. Helly, "Simulation of bottlenecks in single-lane traffic flow," in *Theory Traffic Flow*, R. Herman, Ed. Elsevier, 1959, pp. 207–238.

[4] D. C. Gazis, "Nonlinear follow-the-leader models of traffic flow," *Oper. Res.*, vol. 9, no. 4, pp. 545–567, 1961, doi:10.1287/opre.9.4.545.

[5] M. Bando *et al.*, "Dynamical model of traffic congestion and numerical simulation," *Phys. Rev. E*, vol. 51, no. 2, pp. 1035–1042, Feb. 1995, doi:10.1103/PhysRevE.51.1035.

[6] F. van Wageningen-Kessels *et al.*, "Genealogy of traffic flow models," *Eur. J. Transp. Logist.*, vol. 4, no. 4, pp. 445–473, 2015, doi:10.1007/s13676-014-0045-5.

[7] V. Giammarino *et al.*, "Traffic flow on a ring with a single autonomous vehicle—an interconnected stability perspective," *IEEE Trans. Intell. Transp. Syst.*, vol. 22, no. 8, pp. 4998–5008, 2021, doi:10.1109/TITS.2020.2985680.

[8] S. E. Shladover *et al.*, "Cooperative adaptive cruise control definitions and operating concepts," *Transp. Res. Rec.*, no. 2489, pp. 145–152, 2015, doi:10.3141/2489-17.

[9] S. E. Shladover *et al.*, "Impacts of cooperative adaptive cruise control on freeway traffic flow," *Transp. Res. Rec.*, no. 2324, pp. 63–70, 2012, doi:10.3141/2324-08.

[10] R. E. Stern *et al.*, "Dissipation of stop-and-go waves via control of autonomous vehicles: Field experiments," *Transp. Res. Part C*, vol. 89, pp. 205–221, 2018, doi:10.1016/j.trc.2018.02.005.

[11] Y. Zheng *et al.*, "Smoothing traffic flow via control of autonomous vehicles," *IEEE Trans. Intell. Veh.*, to appear, Dec. 2018, doi:10.1109/JIOT.2020.2966506.

[12] L. Guzzella, *Analysis and Synthesis of Single-Input Single-Output Control Systems*, 4th rev. ed. vdf Hochschulverlag, 2019.

[13] R. E. Kalman, "Mathematical description of linear dynamical systems," *SIAM J. Control Ser. A*, vol. 1, no. 2, pp. 152–192, 1963, doi:10.1137/0301010.

[14] S. Skogestad and I. Postlethwaite, *Multivariable Feedback Control: Analysis and Design*, 2nd ed. Wiley, 2005.

[15] R. M. Gray, *Toeplitz and Circulant Matrices: A Review*, Found. Trends Commun. Inf. Theory, vol. 2, no. 3, pp. 155–239, 2006, doi:10.1561/0100000006.

[16] S. Feng *et al.*, "String stability for vehicular platoon control: Definitions and analysis methods," *Annu. Rev. Control*, vol. 47, pp. 81–97, 2019, doi:10.1016/j.arcontrol.2019.03.001.